Absolute soft x-ray calibration of laser produced plasmas using a focusing crystal von Hamos spectrometer

T. Weeks*[a], M. Harrison[a], M. Johnson[a], A. P. Shevelko[b], J. Ellsworth[a], S. Bergeson[a], M. Asplund[a], L. V. Knight[a]
[a]Physics Department, Brigham Young University, N283 Provo, UT 84602
[b]Lebedev Physical Institute (FIAN), Leninski Pr. 53, Moscow 119991, Russia

ABSTRACT

Absolute x-ray calibration of laser-produced plasmas was performed using a focusing crystal von Hamos spectrometer. The plasmas were created by an *Nd-YAG* laser (0.53 μm/200 mJ/3 ns/10 Hz) on massive solid targets (Mg, Cu, Zn, Sn, Mo, Ta, Ti, Steel). Cylindrical mica crystal (radius of curvature R=20 mm) and a CCD linear array detector (Toshiba model TCD 1304AP) were used in the spectrometer. Both the mica crystal and CCD linear array were absolutely calibrated in the spectral range of λ=7 – 15 Å. The spectrometer was used for absolute spectral measurements and the determination of the plasma parameters. The unique target design allowed for multiple instruments to observe the plasma simultaneously which improved analysis. High spectrometer efficiency allows for the monitoring of absolute x-ray spectra, x-ray yield and plasma parameters in each laser shot. This spectrometer is promising for absolute spectral measurements and for monitoring laser-plasma sources intended for proximity print lithography.

Keywords: laser-generated plasmas, x-ray conversion and spectroscopy, plasma instability

1. INTRODUCTION

Over the past few decades the number of applications and demands for stable x-ray sources have risen along with the number of available sources including: x-ray tubes, laser-produced plasmas, synchrotron facilities, and z-pinch facilities. Synchrotron radiation has become the workhorse of modern x-ray research. Its stability, tunability, and large power output have made it optimal for most scientific applications. Unfortunately, these large facilities do not fit in the lab or within the realm of feasibility for major commercial applications. Because of these major restrictions, laser produced plasmas have become an important alternative. With a peak power comparable to that of a synchrotron source[1], laser-produced plasmas can deliver a very high powered pulse within the Soft X-Ray/EUV wavelength range. This compact and relatively inexpensive source of radiation stands to make considerable advances in a number of areas including Medicine[1], diagnostic research, Homeland Security, EXAFS (extended x-ray absorption fine structure), and next generation lithography.[2,3,4,5]

With next generation lithography perpetually two years away and the industry clamoring to keep up with Moore's law, lithography seems to have the most to gain from such an inexpensive and accessible x-ray source.[6] Possible problems for lithography include the stability of the spectral radiation and debris damage to expensive optics. According to Celliers et al., the specifications that the plasma x-ray source would have to meet can be summarized as follows: the source would have to deliver approximately 15 mJ/cm^2 of x-ray irradiance to the photoresist with a uniformity of 1% over a 3X3 cm^2 area within an exposure interval of approximately 1.3 s. The x-ray spectrum would have to occupy a 20% bandwidth centered on a wavelength of 12 Å.[7] Given existing laser technology, the 1 kW needed to meet these requirements is obtainable.

*ty.weeks@gmail.com; phone 1 801 369-1569

Laser-Generated, Synchrotron, and Other Laboratory X-Ray and EUV Sources, Optics, and Applications II Edited by Kyrala, Gauthier, MacDonald, Khounsary
Proc. of SPIE Vol. 5918, 59180R, (2005) · 0277-786X/05/$15 · doi: 10.1117/12.619632

Downloaded From: http://proceedings.spiedigitallibrary.org/ on 03/18/2014 Terms of Use: http://spiedl.org/terms

The purpose of our research is to improve the spectral analysis of x-rays emitted from laser-produced plasmas and other sources. We performed a calibration and made several spectral measurements. This paper is divided into four main sections. First, in Experimental Methods we will discuss the construction of a novel target system, a basic von Hamos spectrometer, the calibration of the plasma, and the calibration of the spectrometer. Second, in the Results section we will present data that we collected. The Discussion section offers an analysis of the data, spectral stability from shot to shot, and includes an explanation of some anomalous behavior. And finally in the Conclusion section we will briefly discuss current and future research.

2. EXPERIMENTAL METHODS

2.1 The Target

The target was designed to improve the stability and the longevity of the material. The target material was a cylindrical sample mounted on a vertical micron screw which was driven by a stepper motor at the same repetition rate as the laser (figure 1). In this way, as the target turned, it also moved vertically, exposing a new face along the cylinder with each shot. The wobble of the target was measured with a dial indicator to ensure that the face of the material did not move out of the focal spot as it turned. The symmetry of this design also allowed us to mount multiple detectors close to the plasma thereby making several measurements simultaneously.

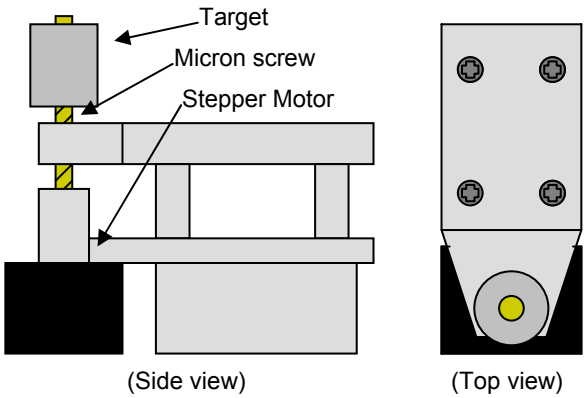


Figure 1: General scheme of novel target system that maximizes the amount of the target used as well as increases the number of instruments that can observer the plasma directly.

2.2 The von Hamos Spectrometer

The von Hamos spectrometer used cylindrically bent mica as a diffraction grating. The mica was mounted over a window cut into the side of a 4 cm diameter brass cylinder, giving the mica a radius of curvature of 2 cm. A Toshiba CCD linear array, used as a detector, was installed in a holder and placed on the axis of symmetry of the cylinder. By Bragg diffraction the von Hamos spectrometer disperses photons along the CCD by wavelength.[8,14] Incident x-rays were focused along the axis of the CCD, as illustrated in figure 2, because of the bent nature of the crystal.

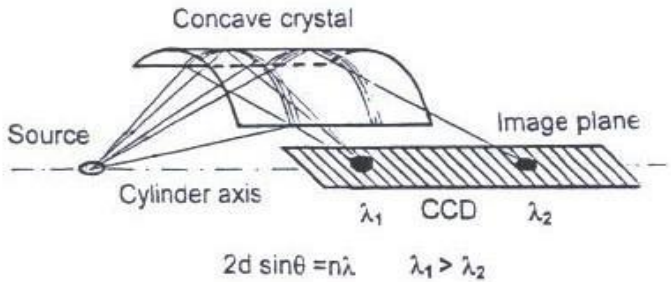


Figure 2: Spectrometer scheme with Bragg diffraction of wavelengths.[14]

Downloaded From: http://proceedings.spiedigitallibrary.org/ on 03/18/2014 Terms of Use: http://spiedl.org/terms

2.3 Calibration of the Plasma

To calibrate the spectrometer we simultaneously observed a laser-produced plasma, created on a Mg target, with a calibrated PIN diode (IRD AXUVHS5) and a von Hamos spectrometer with a linear CCD array (Toshiba TCD1304AP) as the photodetector (see figure 3).The plasma was created using an *Nd-YAG* laser (0.53 μm/200 mJ/3 ns/10 Hz). Both the diode and the CCD were fitted with a 6μm Al filter. Al has an absorption edge just above the w,y resonance and recombination lines and the k,j dielectric satellite lines (Gabriel's notation) of Mg.[12] Because Mg has very few spectral lines and a high characteristic-line to continuum ratio, the Al filter selects a narrow bandwidth that can be considered quasi-monochromatic[13] (see figure 4). Thus, the diode and spectrometer were restricted to monitoring the same wavelength range.

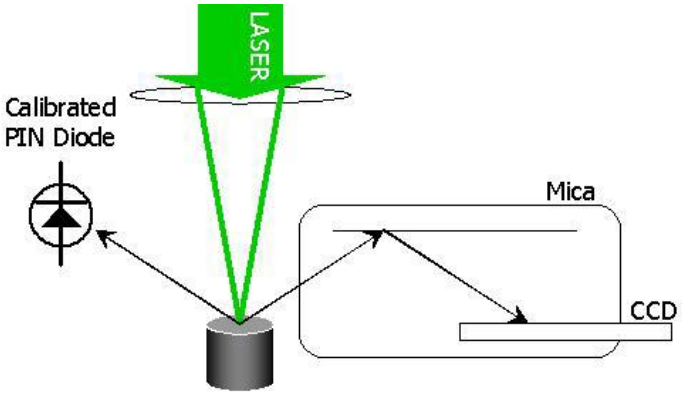


Figure 3: Calibration scheme

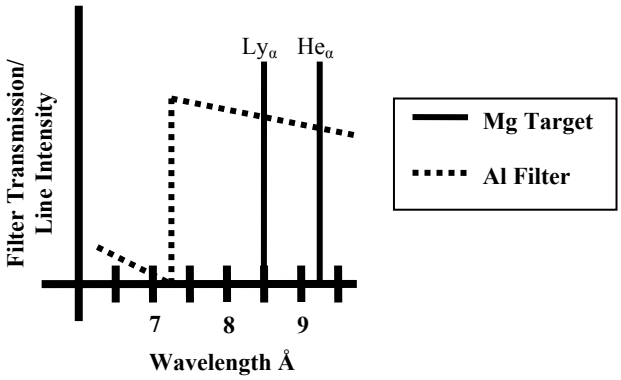


Figure 4: The creation of a quasi-monochromatic source using an Al filter and Mg targert.

The photon intensity incident on the PIN diode along with the solid angle it subtended gave the number of photons per sterradian emitted by the plasma. To determine the yield, I_{diode}, the signal was sent from the diode directly to an oscilloscope (LeCroy Waverunner LT 342). To determine the capacitance of the detector, its time constant τ was determined by observing its exponential waveform with the oscilloscope's input termination set to 1 MΩ. This measurement was then repeated with the termination set to 0.5MΩ. Capacitance was solved for using τ=RC. Since Q=CV, the total charge and subsequently the number of charge carries produced in the diode were determined. Then, based on the diode specifications we were able to determine the number of incident photons per sterradian, I_{plasma}, emitted by the plasma.

Downloaded From: http://proceedings.spiedigitallibrary.org/ on 03/18/2014 Terms of Use: http://spiedl.org/terms

2.4 Calibration of the Spectrometer

The intensity of the spectral lines on the spectrometer was determined by dividing the plasma intensity, I_{plasma} (photons per steradian), by the spectral intensity, $I_{spectrometer}$ (counts per steradian) that was observed on the von Hamos spectrometer (see equation 1). Attenuation due to the Al filters was factored into the calculations.

$$I_{calibrated} = \frac{I_{plasma}}{I_{spectrometer}} \left(\frac{photons}{count} \right) \tag{1}$$

The data coming directly from the CCD only gave intensity, in arbitrary counts, at each pixel on the detector. By multiplying $I_{calibrated}$ by the number of counts at each pixel and using a given dispersion relation[14] (equation 2), the number of incident photons were determined per pixel. Note that neither the integrated reflectivity of the mica or the quantum efficiency of the CCD were taken into account individually but rather the spectrometer was calibrated as a single unit where the quantum efficiency of the PIN diode was used to determine the efficiency of the entire instrument.

$$D_{dispersion} = \left(\frac{2d}{2nR} \sin^2(\theta) \cos(\theta) \right)^{-1} \tag{2}$$

D is the dispersion, R is the radius of curvature of the mica, 2d is the 2d-spacing of the mica, n is the diffraction order, and θ is the angle of incidence of the photon on the mica.

By inserting the known wavelengths of two different reaper lines from a spectrum[15] and the pixel number at which they appeared on the CCD into equation 3 and then solving the two equations simultaneously for A and R, a general equation for λ as a function of pixel number was derived.

$$\lambda_1 = \frac{2d}{n} \sin\left(\cot^{-1}\left(\frac{A_{\mu m} + \#_{pixel} 1 \cdot 8_{\mu m}}{2R_{\mu m}} \right) \right) \tag{3}$$

Where λ is the wavelength of one reaper line, n is the diffraction order, 2d is the 2d-spacing of the mica, θ is the angle of incidence, R is the radius of curvature of the mica, and A is the distance from the source to the edge of the CCD. Since R is already known this method also serves as a good check that the values obtained from the reaper lines of wavelength and pixel number were correct. If the calculated R is accurate then it can also be inferred that the calculated value for A is accurate. Both these values were used to determine the solid angle subtended by the spectrometer and the intensity of any given spectral line observed by the spectrometer

The spectral calibration of various plasmas was performed using a von Hamos spectrometer that was calibrated as described above. The mica and CCD were kept in the same position with respect to the target throughout the experiment to ensure that the same spread of wavelengths were being observed at the same locations along the CCD. By maintaining constant positions of the mica and CCD, accurate spectral composition could be determined for poorly defined spectra. With these absolute spectra the yield of any given wavelength from the plasma could be determined by integrating a desired line across its full-width half-maximum.

3. RESULTS

3.1 X-ray Analysis and Plasma Calibration

The following spectra were taken from Mg (figure 5), Cu (figure 6), Zn (figure 7), Mo (figure 8), Sn (figure 9), Ta (figure 10), Ti (figure 11), and Fe (steel) (figure 12). These plasmas were calibrated in the region of 8-10Å using the calibrated von Hamos spectrometer.

Downloaded From: http://proceedings.spiedigitallibrary.org/ on 03/18/2014 Terms of Use: http://spiedl.org/terms

Spectral information for some of the spectra was difficult to decipher due to the close proximity and large number of spectral lines. To compensate for this line crowding on selected spectra, we applied a Savitzky-Golay filter with a very high polynomial order. The effect of this filter is that high frequency information is eliminated with very little attenuation to the peaks. This filter actually does a poor job at eliminating noise but this was desired since much of the high frequency content was closely spaced spectral lines. The result is a spectrum still carrying much of the original spectral content but with the larger lines much more distinguishable from each other. Spectra in which the Savitzky-Golay filter was used are marked in the figures below.

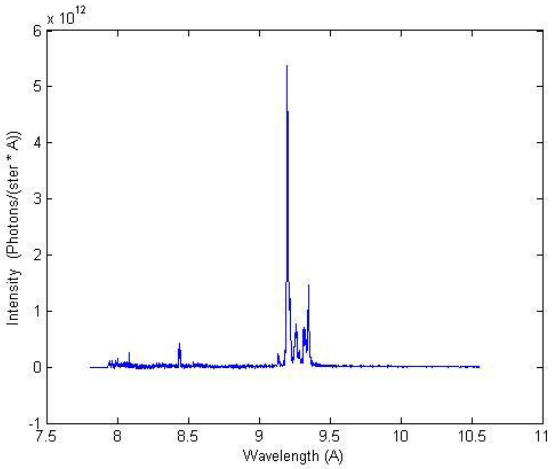


Figure 5: Mg

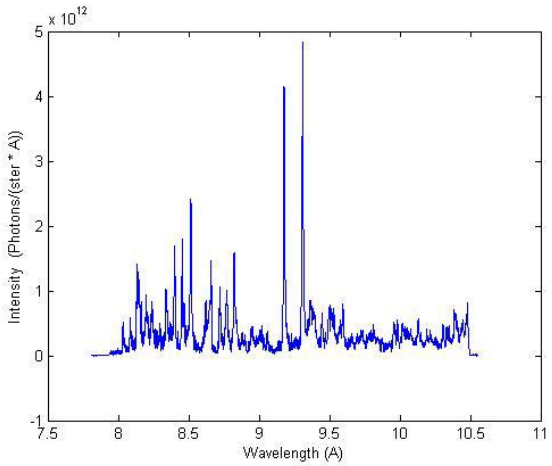


Figure 6: Cu

Downloaded From: http://proceedings.spiedigitallibrary.org/ on 03/18/2014 Terms of Use: http://spiedl.org/terms

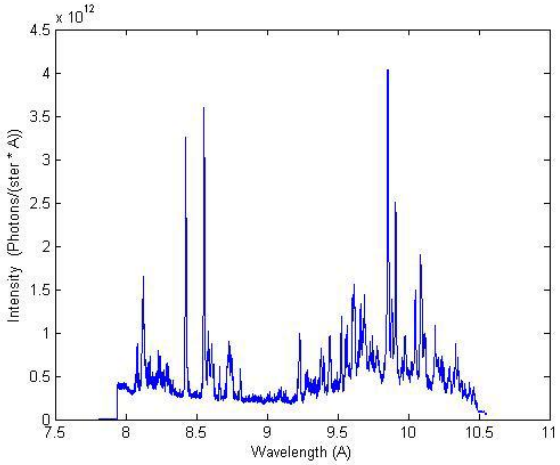


Figure 7: Zn

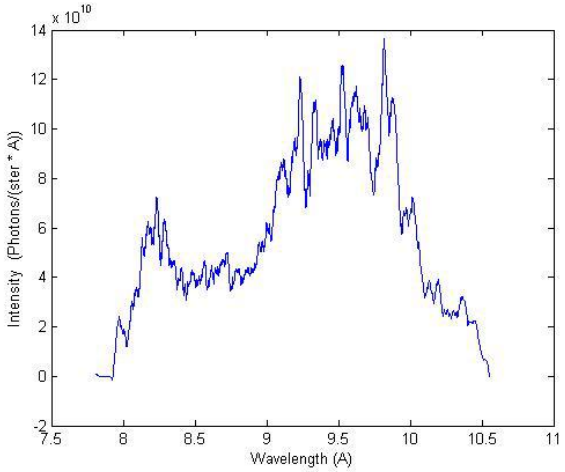


Figure 8: Mo (filtered)

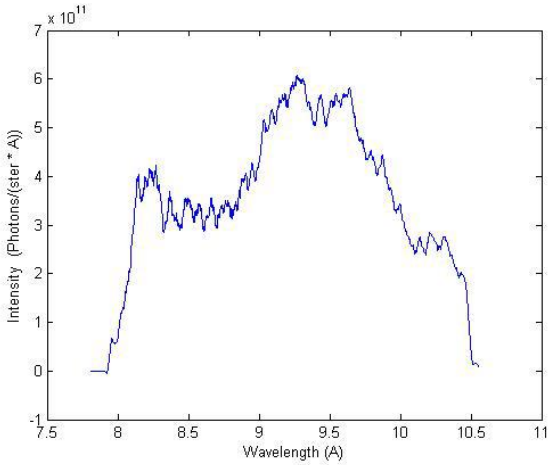


Figure 9: Sn (filtered)

Downloaded From: http://proceedings.spiedigitallibrary.org/ on 03/18/2014 Terms of Use: http://spiedl.org/terms

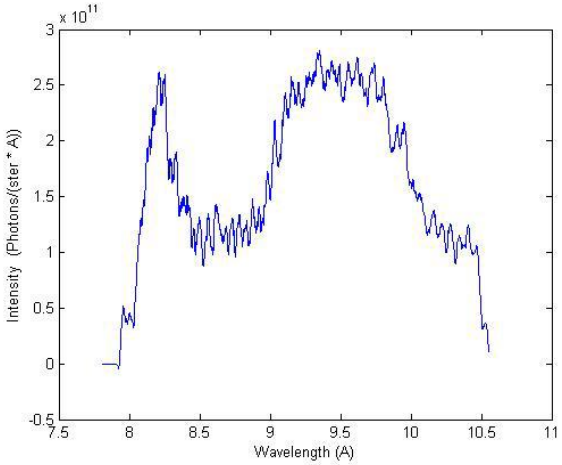


Figure 10: Ta (filtered)

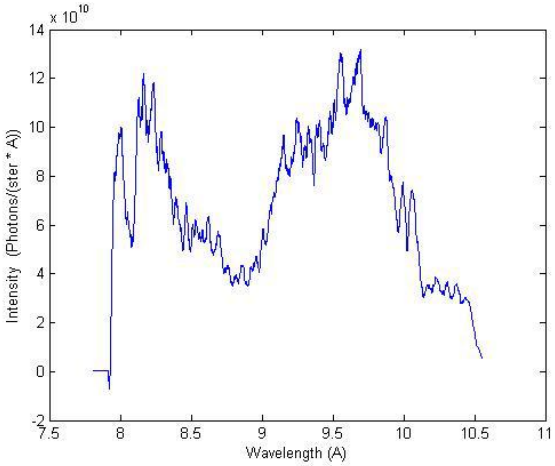


Figure 11: Ti (filtered)

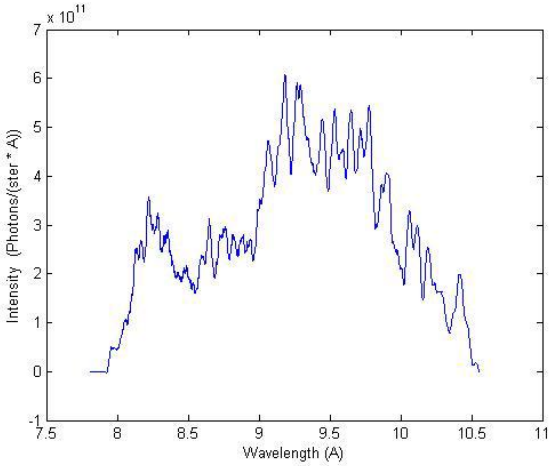


Figure 12: Steel (filtered)

Downloaded From: http://proceedings.spiedigitallibrary.org/ on 03/18/2014 Terms of Use: http://spiedl.org/terms

4. DISCUSSION

4.1 Analysis of recorded spectra

Plasma parameters can be determined by the characteristic lines j, k, w, and y[16,17]. The electron temperature, T_e, can be determined by the ratio j+k/w (the dielectric satellite lines to the resonance line) and the electron density, N_e, can be determined by the ratio w/y (the resonance line to the recombination line)[11,12]. For Mg, T_e and N_e were determined to be 270 eV and $3*10^{20}$ cm^{-3} respectively. These values were very simple to calculate because the relationship between the line ratios and the T_e and N_e are well defined for Mg[11,12]. T_e and N_e for other materials can also be determined since these characteristic lines can easily be identified with this spectrometer. The von Hamos spectrometer when integrated with a CCD has demonstrated spectral resolutions as high as $\lambda/\delta\lambda$= 800, 2000, and 2000 for Mg (1st reflection order), Ti (3rd reflection order), and Fe (5th reflection order) respectively[19]. To demonstrate the detection threshold of the spectrometer we turned the laser energy down until the characteristic lines in a Mg spectrum were reduced in intensity to the same order of magnitude as the dark noise on the CCD. A spectrum was distinguishable down to laser energies as low as 75 mJ (0.53μm/3 ns/1 Hz).

4.2 Spectral stability from shot to shot

While studying these parameters for Mg we became curious about the stability of calibrated plasma. To measure this possible instability we took spectra of ten different plasmas at the lowest laser energy that would produce a plasma (approximately 75 mJ 532 nm) on a Mg target. We then increased the laser energy incrementally, taking ten spectra at each energy, until we reached the maximum output of our laser. We found that x-ray yield of our plasma could vary significantly from shot to shot even at large energies and with constant electron temperature (see figure 13). This instability demonstrates the need for more thorough monitoring of plasma x-ray sources by instruments like the von Hamos spectrometer if laser-produced plasmas are to be use in applications such as lithography. While the focus of our research is not to develop stable plasma x-ray sources, this von Hamos spectrometer could be crucial to researchers who wish to do so.

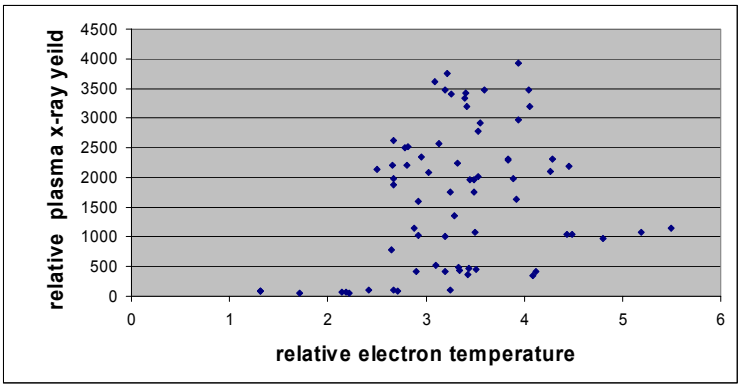


Figure 13: Electron temperature plotted as a function of x-ray yield.

4.3 Anomalous behavior

It should be noted that at about 10 Å all of the data we collected appears to gradually drop to zero. This data does not reflect the actual x-ray emission of the plasma but is an artifact of the penumbral blur of the edge of the spectrometer.

An anomalous attenuation in the region of 8.5-9Å is consistently observed in all our collected data. It was first noticed when we were unable to see the k_α line for Mg (just below 8.5 Å) which is supposed to be comparable to the w resonance line in amplitude but either does not appear or seems to be very attenuated. Several methods were used to improve the signal in that particular region including various geometries (repositioning of both the CCD with respect to the mica as well as repositioning of the spectrometer with respect to the source) and the replacement of several components including the CCD and the mica. As can be observed from the data, this artifact persisted for all of the materials analyzed as a dip in spectral intensity.

Three factors may be contributing to this attenuation. First, according to Ziyu Wu *et al*[21], mica can have a substantial mass absorption coefficient in this spectral region which can be minimized by using an optimized synthetic mica instead

Downloaded From: http://proceedings.spiedigitallibrary.org/ on 03/18/2014 Terms of Use: http://spiedl.org/terms

of the natural mica we use. Second, we did not take into account absorption due to air in the vacuum chamber. All experiments were performed at a pressure of 300 mTorr of air. This pressure was preferred over a much higher vacuum to speed up the process of changing samples and making adjustments to equipment. While the air in the chamber is not likely to exhibit such a narrow absorption edge it may be affecting the development and expansion of our plasma. Third, there may be some intrinsic problem in the anomalous spectral region that is built into the type of CCD we have chosen as a detector. Although we have not been able to satisfactorily characterize the anomaly it does not lie within the desired bandwidth for x-ray lithography (10-14Å)[7]; so for application purposes it is of secondary concern.

5. CONCLUSSION

We have calibrated laser-produced plasmas from several materials using a compact von Hamos spectrometer which was calibrated to determine absolute x-ray intensity within a spectral range of 8-10Å. X-ray plasma emission was observed to be unstable from shot to shot, demonstrating the necessity for continuous monitoring of such x-ray sources. Future research includes the calibration of a conical von Hamos spectrometer that can be positioned much further from the source and therefore minimize debris damage to the mica crystal.

6. ACKNOWLEDGMENTS

We would like acknowledge Brigham Young University for its support.

7. WORKS CITED

1. E. Förster, R. Butzbach, P. Gibbon, J. Uschmann, H. Daido, K. Fujita, and H. Nishimurab, “Diagnostics and applications of laser produced plasmas” *SPIE* Vol. **3886**, p. 342-352, 2000.
2. A.J. Bourdillon, C. B. Boothroyd, **“**Proximity correction simulations in ultra-high resolution x-ray lithography” J. Phys. D: Appl. Phys. **34**, p. 3209-3213, 2001.
3. J. Bourdillon, C. B. Boothroyd, G. P. Williams, and Y. Vladimirsky, “Near field x-ray lithography simulations for printing fine bridges” J. Phys. D: Appl. Phys. **36**, p. 2471-2482, 2003.
4. J. Bjorkholm, “EUV Lithography - The successor to optical lithography?” Intel Technology Journal **Q3**, 1998.
5. H. Smith, and M. L. Schattenburg, “X-ray lithography, from 500 to 30 nm: X-ray nanolithography” IBM J. Res. Develop. **31**, No. 3, 1993.
6. K. Derbyshire, “Next-Generation Lithography: Beyond 100 nm” Semiconductor Magazine. **2**, No. 9, 2001.
7. P. Celliers, L. B. DaSilva, C. B. Dane, S. Mrowka, M. Norton, L. Hackel, D. Matthews J. R. Maldonado, and J. A. Abate, “Optimization of x-ray sources from a high average power ND:Glass laser-produced plasma for proximity lithography” ICF Annual Report. p. 157-167, 1995.
8. L. V. Hamos, Z. Kristallog, “Formation of true x-ray images by reflection on crystal mirrors” **101**, p. 17-29, 1939
9. P. Beiersdorfer, and J. R. Crespo Lopez-Urrutia, et al., “Very high resolution soft x-ray spectrometer for an electron beam ion trap” Rev. Sci. Instrum. **68**, p. 1077-1079, 1997.
10. Robert R. Whitlock, et al., “X-ray Spectral Measurements of the JMAR High Power Laser-plasma Source” *SPIE* Vol. **4781**, p. 35-41, 2002.
11. L.P. Presnyakov, “X-ray spectroscopy of high-temperature plasma” Usp. Fiz. Nauk **119**, p. 49-73, 1976.
12. L. A. Vainshtein, U. I. Safronova, and A. M. Urnov, "Dielectronic satellites of resonance lines of highly charged ions," Proceedings of the Lebedev Physical Institute, Nova Science publishers, ed. N. G. Basov, 119, 1980.
13. A. P. Shevelko, I. Beigman, and L. V. Knight, “Formation of quasi-monochromatic soft x-ray radiation from laser-produced plasmas” *SPIE* Vol. **4781**, p. 10-16, 2002.
14. A.P. Shevelko, “X-ray spectroscopy of laser-produced plasmas using a von Harnos spectrograph” *SPIE* Vol. 3406, pp. 91-108, 1998.
15. V. A. Boiko, A. Ya. Faenov, and S. A. Pikuz, “X-ray spectroscopy of multiply-charged ions from laser plasmas” J. Quant. Spectrosc. Radiat. Transfer. **19**, p. 11-50, 1976.
16. D. Porquet, and J. Dubau, “X-ray photoionized plasma diagnostics with helium-like ions: Application to warm absorber-emitter in active galactic nuclei” Astron. Astrophys. Suppl. Ser. **143**, p. 495-514, 2000.
17. A.V. Vinogradov, I. Yu. Skobelev, and E.A. Yukov, “Determination of plasma density from spectra of helium-like ions” Sov. J. Quant. Electron. **5**, 1975

Downloaded From: http://proceedings.spiedigitallibrary.org/ on 03/18/2014 Terms of Use: http://spiedl.org/terms

18. C. Biedermann, R. Radtke, and K. B. Fournier, "Spectroscopy of heliumlike argon resonance and satellite lines for plasma temperature diagnostics" Phys. Rev. E. **66**, 066404, 2002.
19. A. P. Shevelko,Yu. S. Kasyanov, O. F. Yakushev, L. V. Knight, "Compact focusing von Hamos spectrometer for quantitative x-ray spectroscopy," Rev. Sci. Instrum., **73**, 3458-3463, 2002.
20. L. Beigman, P. Ya Pirogovskiy, L. P. Presnyakov, A. P. Shevelko and D. B. Uskov, "Interaction of a laser-produced plasma with a solid surface: soft x-ray spectroscopy of high-Z ions in a cool dense plasma" J. Phys. B: At. Mol. Opt. Phys. **22** (1989) 2493-2502.
21. Ziyu Wu, A. Marcelli, G. Cibin, A. Mottana, and G. Della Ventura, "Investigation of the mica x-ray absorption near-edge structure spectral features at the Al K-edge" J. of Physics: Condensed Matter. **15**, p. 7139-7148, 2003.

Downloaded From: http://proceedings.spiedigitallibrary.org/ on 03/18/2014 Terms of Use: http://spiedl.org/terms